THE ASTRONOMICAL JOURNAL, 118:1120–1125, 1999 August

COMET HALE-BOPP (C/1995 O1) NEAR 2.3 AU POSTPERIHELION: SOUTHWEST ULTRAVIOLET IMAGING SYSTEM MEASUREMENTS OF THE H_2O AND DUST PRODUCTION

S. ALAN STERN, WILLIAM B. COLWELL, MICHEL C. FESTOU, PETER M. TAMBLYN, AND JOEL WM. PARKER
Southwest Research Institute, Suite 426, 1050 Walnut Street, Boulder, CO 80302

DAVID C. SLATER
Southwest Research Institute, 6220 Culebra Road, P.O. Drawer 28510, San Antonio, TX 78238

PAUL R. WEISSMAN
Jet Propulsion Laboratory, 4800 Oak Grove Drive, Pasadena, CA 91109

AND

LARRY J. PAXTON
Applied Physics Laboratory, Johns Hopkins University, 11100 Johns Hopkins Road, Laurel, MD 20723
Received 1999 January 27; accepted 1999 April 22

ABSTRACT

The Southwest Ultraviolet Imaging System (SWUIS) imaged comet C/1995 O1 (Hale-Bopp) in various bandpasses from the Space Shuttle on nine occasions during 1997 August 9–15. These observations occurred when the solar elongation of the comet was too small to permit *Hubble Space Telescope* and other UV observations. Here we present some first results of the continuum and gas emission measurements collected by SWUIS. We find that Hale-Bopp's dust-production parameter, $Af\rho$, was $(2.0 \pm 0.8) \times 10^5$ cm when the comet was 2.33 AU from the Sun. Furthermore, we find that its water production rate, $Q(H_2O)$, was $(2.6 \pm 0.4) \times 10^{29}$ s^{-1}. Combining this result with both other published H_2O production rates and CO production rates, we find that our measurements were made at the beginning of the period when the comet's activity was in transition from a H_2O dominated to a CO-dominated state. We also find that the average rate of decrease of the water production between perihelion and 2.33 AU postperihelion was very close to $r_h^{-4.0 \pm 0.6}$, but concerns over radio data indicate that it may have been shallower immediately postperihelion and then considerably steeper beyond about 2 AU. Such a behavior could indicate a sharply declining H_2O production rate beyond 2 AU, but if this is the case, then the H_2O production curve's steepening and turnoff occurred ≈ 1 AU closer to the Sun postperihelion than did the H_2O turn-on preperihelion. An alternative explanation could be that a seasonal (i.e., obliquity-dependent shadowing) effect may have caused a reduction in illuminated area on Hale-Bopp's irregular nucleus between 1.5 and 2.3 AU outbound.

key words: comets: general

1. INTRODUCTION

The study of comets in the ultraviolet has been a highly productive pursuit (e.g., Feldman 1982, 1991; Festou, Rickman, & West 1993a, 1993b; Stern 1999). Comet Hale-Bopp (C/1995 O1) presented solar system astronomers with a spectacular opportunity to study a high-activity comet in this way. We took advantage of this opportunity by proposing to fly our UV imager, the Southwest Ultraviolet Imaging System (SWUIS; see Slater et al. 1999), aboard the Space Shuttle. The primary objective of this mission was to provide a unique set of OH and UV continuum measurements by observing Hale-Bopp at some point during the long, almost 9 month period surrounding the comet's 1997 April 1 perihelion, when the comet would be at too small a solar elongation angle (SEA) to be observed by UV instruments aboard the *Hubble Space Telescope* (*HST*).

Although not specifically designed for cometary observations, SWUIS has certain attributes that make it useful for this purpose; these include a comparatively wide field of view (FOV) (adjustable from 0°.1 to 0°.6 with the telescope; up to 12° can be achieved using a lens instead of the telescope), high temporal resolution (60 Hz), and the capability to observe objects at SEAs as low as 17°.[1]

SWUIS flew its first mission aboard STS-85 in 1997 early August, with the objective of obtaining images of Hale-Bopp in various bandpasses from 2500 to 8500 Å. The experiment performed flawlessly, and some 4.3×10^5 images of the comet were obtained. Here we report our first results. These involve a small fraction of the SWUIS data set, centering on the determination and interpretation of H_2O and dust production measurements of the comet at 2.3 AU. Future reports are planned once more analyses have been completed, with the intent of exploring OH and continuum-band image morphologies and color-dependent $Af\rho$ measurements.

2. INSTRUMENT OVERVIEW

SWUIS is a mid-UV/visible instrument capable of imaging astronomical targets in any filter bandpass

[1] SWUIS was in fact designed, and was initially selected, to fly on the Shuttle to obtain photometry and spectroscopy of Venus, Mercury, and the Jovian system; these observations have been delayed owing to Shuttle scheduling, but are now set to begin in 1999 July aboard STS 93.

TABLE 1

SWUIS HALE-BOPP OBSERVATION SUMMARY

SWUIS Orbit	Date	Imaging Filters
STS 85-1......	1997 Aug 09	Green continuum, OH, H_2O^+, CO^+
STS 85-2......	1997 Aug 09	CS, UV continuum, C_2, CN, OH
STS 85-3......	1997 Aug 12	OH, CN, C_2, broadband visible continuum
STS 85-4......	1997 Aug 12	Broadband UV, H_2O^+
STS 85-5......	1997 Aug 14	OH, UV continuum, broadband visible continuum
STS 85-6......	1997 Aug 14	OH, UV continuum, broadband visible continuum
STS 85-7......	1997 Aug 14	OH, CN, C_2, broadband visible continuum
STS 85-8......	1997 Aug 15	OH, UV continuum, broadband visible continuum
STS 85-9......	1997 Aug 15	OH, UV continuum, broadband visible continuum

throughout the 2500–8500 Å region.[2] The imager + electronics system is fed by an 18 cm aperture, fused silica/MgF_2 UV-Maksutov telescope with an adjustable focal length (1.05–2.57 m). The telescope feeds an optical coupler capable of housing up to three filters in series, which in turn feeds one of two image-intensified CCDs (ICCDs). The two ruggedized SWUIS ICCDs are sensitive to the visible (>30% DQE 4000–8500 Å, peak at 6500 Å) and the UV (>20% DQE 2000–6500 Å, peak at 3500 Å). The cameras can operate in either manual or automatic gain modes, and have a 370 × 420 pixel format. The ICCDs frame at 60 Hz, allowing us to coregister and co-add images to remove low-level attitude dead-band jitter and drift. SWUIS data are recorded using a standard on-board Shuttle video interface; data can also be transmitted to the ground in real time for diagnostic purposes. Filters can be changed out to select various bandpasses, as desired.

SWUIS is specifically designed to operate as a Shuttle in-cabin instrument. The Shuttle cabin has 10 windows; of highest utility is the optical-quality UV-transmissible

[2] Flights 2 and 3 will enhance these capabilities by extending the bandpass to 1.1 μm, doubling sensitivity, adding a subarcsecond high-resolution mode, and adding a long-slit, Rowland circle spectrograph facility.

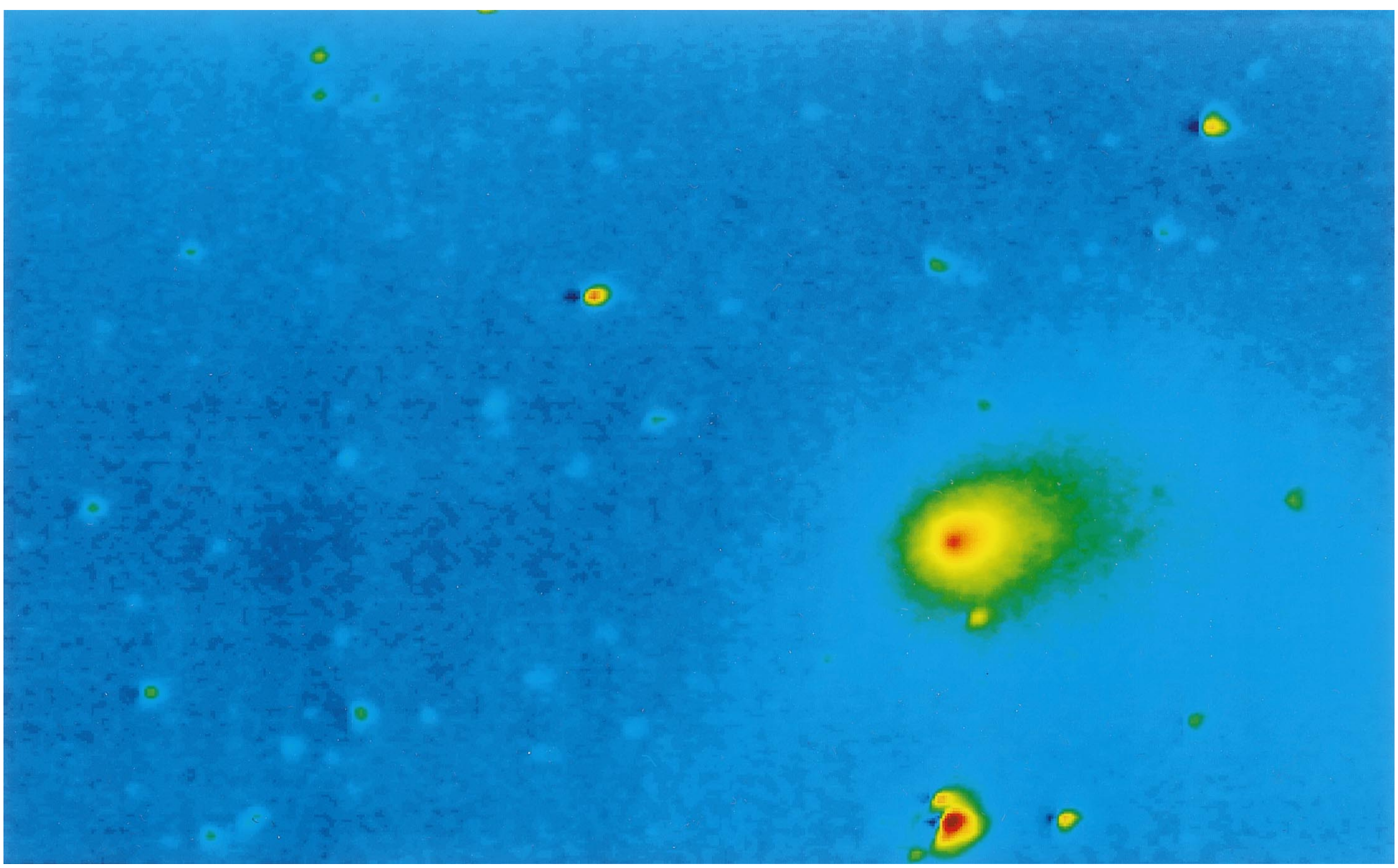

FIG. 1.—Direct co-add of 30 s of SWUIS Hale-Bopp data made with the clear filter on 1997 August 13. The field shown measures 0°.45 × 0°.34 and represents a "raw" data product: the 1800 images used in this co-addition were not coregistered during co-addition, and the resulting image has been neither calibrated nor flat-fielded. In addition to Hale-Bopp (total visual magnitude 4.7), field stars as faint as $V = 11.5$ are also visible here.

window on the middeck of each vehicle. This window has greater than 70% transmission from 2200 Å to almost 2 μm. SWUIS observations are obtained by dedicated pointings scripted into the Shuttle's attitude time line. Coarse pointing is achieved through Shuttle attitude control, and fine pointing is adjusted via a pivot joint in the instrument's two-axis window mount.

3. HALE-BOPP OBSERVATIONS AND DATA SET

SWUIS was launched aboard the Shuttle Discovery on 1997 August 8.[3] The mission extended over 1997 August 8–17. SWUIS imaging runs were obtained on August 9, 12, 14, and 15. The mean heliocentric distance, heliocentric velocity, and geocentric distance of Hale-Bopp at the time of the observations were 2.33 AU, 21.4 km s^{-1}, and 2.93 AU, respectively. The image plate scale selected for the Hale-Bopp observations maximized the FOV ($\phi = 0\overset{\circ}{.}6$) at the expense of spatial resolution. The data have been frame-grabbed for the analysis that follows in a 320 × 240 pixel format, yielding an effective scale of $8\overset{''}{.}7$ pixel^{-1}, or 1.86×10^4 km pixel^{-1} in the plane of the sky.

SWUIS observed comet Hale-Bopp on nine orbits during STS-85. The timing and content of these nine SWUIS data takes are summarized in Table 1. The filters used were primarily those contained in the standard Hale-Bopp filter set (see Millis, Schleicher, & Farnham 1997; Farnham & Schleicher 1999).[4]

In the discussion that follows we consider only the OH data obtained on 1997 August 12 and the clear-filter continuum images ($\lambda_c = 5450$ Å) obtained on 1997 August 16. These include some 6000 OH frames, which we co-added for analysis of the comet's water production rate, $Q(H_2O)$, and some 20,000 broadband continuum frames, which we combined to obtain a measure of the comet's dust production. Figure 1 depicts a sample of unprocessed continuum data.

4. DATA REDUCTION

As noted previously, SWUIS data frames are taken at a 60 Hz rate. This data stream is later spatially coregistered, and then co-added to enhance the signal-to-noise. Background stars in the frames are used to accurately coregister the images. As a part of the co-addition process, the data are median-filtered in small groups (during which image jitter is negligible) to remove video noise. Video banding is removed via a combination of FFT filtering and removing the average background trend in the image along each axis. Instrumental dark counts, determined in flight with a dark slide, were subtracted from each co-added image. Each resulting co-add in a given filter bandpass was then flat-fielded using a laboratory flat field determined by measurements of a uniformly illuminated flat screen.

The effective sensitivity of any given SWUIS observation depends on both the instrument response and the Shuttle UV window transmission. Because this window obtains a thin film resulting from launch debris and space exposure, it is preferable to employ an in-flight calibration rather than a laboratory calibration pre- or postflight. Instrument sensitivity was therefore measured in flight by comparing image counts for background stars of known spectral type and distance identified in the images to their estimated flux in the filter bandpass used for the given observation. Background-subtracted stellar flux in a given image co-add was measured using standard aperture photometry techniques. Calibration stars were identified using the on-line SIMBAD star catalog. We relied on HD 59934 for the OH data (B2 III/IV, $m_V = 8.0$) and HD 60626 for the continuum data (G3/G5 V, $m_B = 9.6$), and normalized their known magnitudes and reddening to Kurucz models (Kurucz 1992) for each star. We point out that because SWUIS measurements are made above the Earth's atmosphere, flux uncertainties due to atmospheric absorption of the stellar spectral energy distribution are zero.

5. DERIVED DUST MEASURE

We now turn to the subject of Hale-Bopp's dust production at 2.33 AU, using the $Af\rho$ formulation as a measure (A'Hearn et al. 1984),

$$Af\rho = \left(\frac{F_{\rm comet}}{F_{\odot}}\right)\left(\frac{2r_h\Delta}{\rho}\right)^2 \rho \ , \qquad (1)$$

where $F_{\rm comet}$ is the flux received from the comet by the instrument, $F_{\odot}$ is the solar flux at 1 AU convolved with the effective transmission function of the instrument, r_h is the comet's heliocentric distance (in AU), ρ is the radius of integration of the continuum flux, and Δ is the geocentric distance of the comet.[5]

We calculated the $Af\rho$ result from the co-addition of 20,000 broad bandpass (2500–8500 Å) images, assuming all of the light (after background subtraction) is due to the continuum (i.e., dust). Since Hale-Bopp was particularly dusty, this is a good approximation, but it is, strictly speaking, an overestimate by a factor of $\approx$10%. The comet flux was obtained by integrating over a circular FOV centered on the comet superposed on the image, with a radius of 5 pixels, corresponding to $\rho = 9.20 \times 10^4$ km.

We derive log ($Af\rho$ cm) = 5.30 ± 0.15 when Hale-Bopp was 2.3 AU from the Sun, a record among all comets at this distance. The Weaver et al. (1999) *HST* team found log ($Af\rho$ cm) = 5.09 ± 0.2 at 1″ from the comet and at an effective wavelength of 6500 Å, when Hale-Bopp was 2.48 AU from the Sun. These two results are in excellent agreement, and reconfirm the high dust production of comet Hale-Bopp. Typical long-period comets have log ($Af\rho$ cm) values in the range 2.5–4 (A'Hearn et al. 1995); in the next section, after deriving the water production rate for Hale-Bopp at 2.33 AU, we compare its log $[Af\rho/Q(H_2O)]$ to other comets.

6. DERIVED H_2O PRODUCTION RATE

We used the vectoral model (Festou 1981) to derive water production rates from the OH 0–0 band brightness (see also

[3] Originally, we had hoped to conduct these observations near perihelion at the end of 1997 March, but Shuttle programmatic constraints precluded that possibility.

[4] See also http://www.lowell.edu/users/farnham/hb/hbfilters/index.html.

[5] We note that the user of equation (1) must be careful, in that whereas the units on r_h must be in AU, the units in Δ/ρ can be anything, so long as they are homogenous; then the second ρ outside the parenthesis sets the units for $Af\rho$ itself.

Budzien, Festou, & Feldman 1994). In the model, the lifetimes at 1 AU for H_2O (86,280 s total, 116,300 s dissociative) and OH (142,000 s total) were calculated for the solar activity level for 1997 August, according to the procedure described in Budzien et al. (1994). The solar minimum OH (0–0) zero velocity g-factor at 1 AU was corrected to Hale-Bopp's heliocentric velocity (see Schleicher & A'Hearn 1988),[6] yielding 9.4×10^{-4} s^{-1}; this 1 AU value was then propagated to the heliocentric distance of Hale-Bopp. The value of Hale-Bopp's H_2O parent velocity determined by Colom et al. (1999), $v_p = 1.045/r_h^{1/2}$ km s^{-1}, was adopted for the model calculations presented below.[7]

The comet center was located in OH from the two-dimensional moments of the center of light around the cometary emission peak. The average OH brightness was calculated over the central 5 × 5 pixels (43″ × 43″). A background level was determined for the data using an average value of image brightness measured far in the antisolar direction from the comet. By scaling the measured-continuum flux to the OH flux, and adjusting for both the relative equivalent widths of the two filters and the integrated solar flux in each filter, one easily derives that the continuum contribution to the OH band images of Hale-Bopp must be at or below the 4% level and can be neglected for our purposes.

The observed OH brightness is 6.7 ± 1.1 kR in the co-added images. This brightness yields optically thin column densities, from which we derived $Q(H_2O) = 2.6 \pm 0.4 \times 10^{29}$ molecules s^{-1} at 2.33 AU. This value is in very close agreement with the $Q(H_2O) = 2.4 \pm 0.2 \times 10^{29}$ s^{-1} obtained later by Weaver et al. (1999) using *HST* when Hale-Bopp was at a heliocentric distance of 2.48 AU; indeed, the agreement is so close, given the estimated error bars and the difference in Hale-Bopp's heliocentric distance, that the degree of formal agreement appears remarkable indeed.

In agreement with Weaver et al. (1999), our H_2O sublimation model estimates indicate that between 2% and perhaps 20% of Hale-Bopp's nucleus was actively releasing water, depending on the assumed temperature distribution on the surface; active fractions of less than 5% are rare in comets (A'Hearn et al. 1995).

We now turn to the "big picture" view that the various data sets imply regarding Hale-Bopp's postperihelion behavior. Figure 2 shows both the SWUIS and *HST* $Q(H_2O)$ postperihelion measurements, as well as the radio determinations of $Q(H_2O)$; Figure 2 also shows preperihelion $Q(H_2O)$ data derived from radio measurements. With regard to $Q(H_2O)$, note that the only postperihelion radio observations ($\lambda = 18$ cm) yielded H_2O production rates of 3.5×10^{30} and 2.1×10^{30} s^{-1} at 1.64 and 1.84 AU, respectively (Colom et al. 1999); Hale-Bopp moved rapidly southward thereafter, and no further radio measurements were made.

Combining our $Q(H_2O)$ results with the perihelion water production rate of $(1.2 \pm 0.9) \times 10^{31}$ for Hale-Bopp (Colom et al. 1999), as shown in Figure 2, we find that the average rate of decrease of the water production between perihelion and 2.33 AU postperihelion is about $r_h^{-4.0 \pm 0.6}$; a similar analysis using the *HST* data obtained at 2.48 AU gives $r_h^{-3.8 \pm 0.3}$. Hale-Bopp's average postperihelion rate of decrease of water production, derived from these two results, is thus quite typical of that observed in other old, long-period comets (A'Hearn et al. 1995), which have an average of $r_h^{-3.77}$. The fact that Hale-Bopp's water production rate decrease is typical gives a strong indication that Hale-Bopp's nucleus was not entirely outgassing.

One interesting point about the $Q(H_2O)$ values is that they are very comparable to the $Q(CO)$ values derived by submillimeter techniques in a similar range of r_h (Colom et al. 1999), indicating that Hale-Bopp's activity evolved from being H_2O-dominated inside ≈2.5 AU to being CO-dominated beyond 3.5 AU [see Fig. 2; compare the blue line, postperihelion $Q(CO)$ data to the thick red line depicting $Q(H_2O)$]. It is also interesting to note that preperihelion, the CO-to-H_2O activity evolution occurred about 1 AU farther out, near 3.4 AU (Biver et al. 1997), as shown in Figure 3.

However, inspecting the thick red line in Figure 2, one sees that in order to connect the postperihelion radio and UV points, one requires a distinct change in the water production rate dependence on heliocentric distance somewhere between 1.6 and perhaps 2.0 AU. To make this finding more quantitative, note that from perihelion through 1.84 AU, 18 cm radio measurements correspond to

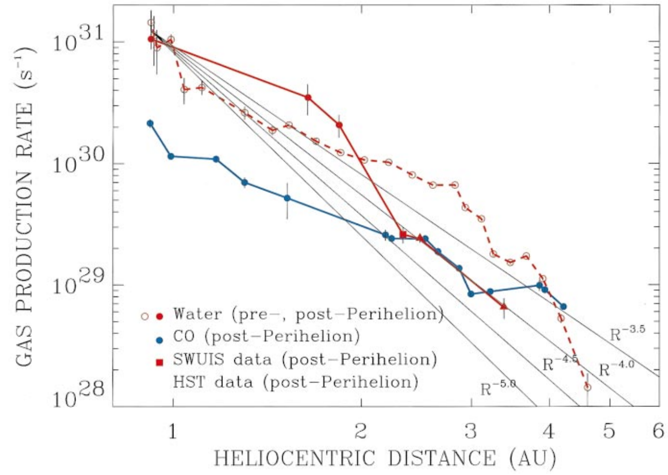

FIG. 2.—Comparison between various determinations of the H_2O and CO production in Hale-Bopp, along with various power-law projections of the OH falloff rate from perihelion. The SWUIS UV $Q(H_2O)$ data point, derived from OH measurements, is shown as the square box at 2.33 AU. The *HST* UV $Q(H_2O)$ point, also derived from OH measurements, is shown as the triangle at 2.48 AU. All other H_2O and CO data are radio measurements. The radio $Q(H_2O)$ results shown here were collected at Nançay by the Meudon team (see Colom et al. 1999); the postperihelion CO data are from Biver et al. (1999); error bars shown are those quoted by the authors. Note that although millimeter-wave observations of CO were made postperihelion when the comet plunged southward, the lack of large radio telescopes in the southern hemisphere prevented OH observations [and therefore $Q(H_2O)$ results] from being obtained. The SWUIS and *HST* UV observations are in excellent agreement with each other, and indicate that either the water production significantly decreased after the last radio observation was collected or the radio determinations are in error due to uncertainties in OH inversion parameter calculations, as noted in the text. Whatever the actual uncertainty in the radio determination, the water production in Hale-Bopp was approximately comparable to the CO production from 2.2 to 3.2 AU postperihelion.

[6] This g-factor has the same value for the quenched and unquenched cases (D. G. Schleicher 1998, private communication).

[7] In contrast, Weaver et al. (1999) used a parent velocity of $v_p = 0.80/(r_h)^{1/2}$ km s^{-1} in their analysis of small-FOV *HST* data. Adopting our v_p relation would reduce the Weaver water production rate values by a factor of $0.8/1.045 = 0.766$.

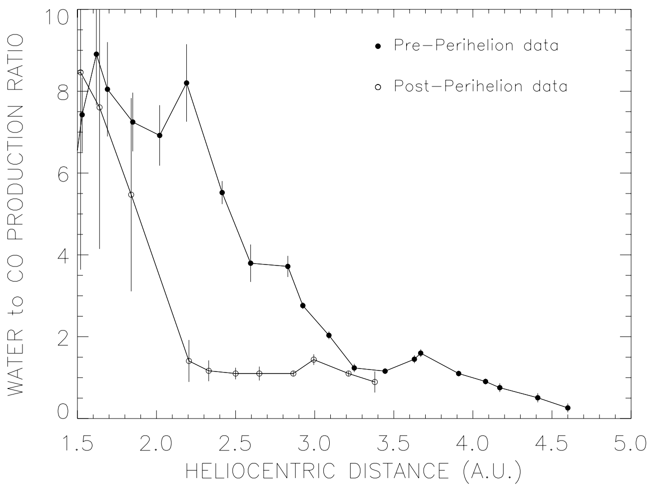

FIG. 3.—Ratio of the radio-derived production of H_2O and CO production rates shown in Fig. 2 for comet Hale-Bopp, both pre- and postperihelion, when the comet was greater than 1.5 AU from the Sun. One sees from this figure that the H_2O production was larger than that of CO between about 3.2 AU preperihelion and about 2.2 AU postperihelion, and that the pre- and postperihelion H_2O/CO production rate curves, when ratioed, are different, displaying an inward offset for the postperihelion branch, as mentioned in the text. Beyond about 4 AU, both preperihelion and postperihelion, the production of H_2O is highly limited by the nucleus temperature, whereas CO can still sublimate in significant amounts.

an H_2O production falloff rate of $r_h^{-2.3 \pm 0.3}$; to accommodate these points with the SWUIS and *HST* UV data, the decline in H_2O production of Hale-Bopp must have then steepened to a value near $r_h^{-7.2 \pm 0.6}$ as the comet moved outward to 2.4 AU.[8]

What could this mean? Such a steepening of the water production rate might be expected at the time of the H_2O production turnoff, but we must note that if this is the case, then as shown by Figure 3, the H_2O production curve's steepening and turnoff occurred ≈ 1 AU closer to the Sun postperihelion than did the H_2O turn-on preperihelion.

One alternative physical mechanism could be a seasonal (i.e., obliquity-dependent shadowing) effect, which may have caused a reduction in active area on Hale-Bopp around the time it reached 1.6–1.8 AU.

Another possibility is that the radio-derived $Q(H_2O)$ points at 1.64 and 1.84 AU may be high owing to uncertainties in the OH inversion parameter i (see Despois et al. 1981) used by Biver et al. (1999). For comparison, Biver et al. used the value $i = 0.03$ (calculated by Schleicher & A'Hearn 1988), but Colom et al. (1999) used Despois's higher value of $i = 0.13$; M. C. Festou & J.-M. Zucconi (1998, private communication) have independently calculated $i = 0.06$ for the same heliocentric velocity, $+21$ km s^{-1}. Proportionately higher values of i lower $Q(H_2O)$ proportionately; so, for example, $i = 0.13$ would lower the radio-derived $Q(H_2O)$ values by a factor of almost 4, which would make the radio-derived results consistent with a single-valued power law from perihelion all the way to the two UV-derived $Q(H_2O)$ determinations.

[8] We note that the preperihelion results of Weaver et al. (1999) do show that the *HST* (UV) water production rates are systematically below the radio results inside 3 AU, thereby leading to the conclusion that some might find it not unexpected that postperihelion UV-derived $Q(H_2O)$ results would also fall below the radio-derived $Q(H_2O)$ results.

7. CONCLUSIONS

We obtained a large data set of visible and UV images of comet Hale-Bopp using the SWUIS UV/VIS imager during Space Shuttle mission STS-85 in 1997 August. At this time the comet was 2.33 AU from the Sun and at a solar elongation angle that prevented other UV (and indeed many visible) instruments from obtaining data. These measurements were made at a time when the H_2O and CO production rates were comparable.

In this report, we have described the SWUIS instrument and its Hale-Bopp data set, and derived H_2O and dust-production measures obtained from these data. We found that Hale-Bopp's dust-production parameter, $Af\rho$, was $(2.0 \pm 0.8) \times 10^5$ cm when the comet was 2.33 AU from the Sun. Furthermore, we found that Hale-Bopp's $Q(H_2O)$ was $(2.6 \pm 0.4) \times 10^{29}$ s^{-1} at this point. We found from the $Q(H_2O)$ determination that between 2% and 20% of Hale-Bopp's nucleus was active at any given time.

The SWUIS-derived $\log [Af\rho/Q(\mathrm{OH})] = -24.1$ shows that Hale-Bopp continued to be highly dusty (by a factor of order 10 to 20) compared with typical comets (see A'Hearn et al. 1995), both in absolute terms and compared with its water-production rate, as it receded from the Sun and its activity declined. Comparing the dust/water production ratio at the time of our postperihelion measurements to a similar result obtained preperihelion at 2.48 AU (Schleicher & Farnham 1997), we find that in absolute terms, the comet was releasing about as much dust pre- and postperihelion, but that in relative terms the comet was dustier postperihelion at 2.3–2.5 AU than in the same heliocentric range preperihelion, owing to reduced water production.

Together, our $Q(H_2O)$ determination and the one made by *HST* at 2.48 AU demonstrate that either the radio-derived $Q(H_2O)$ results shown in Figure 2 are too high, or the comet's behavior changed as a result of seasonal or other effects that caused its water production rate to begin declining more steeply after ≈ 1.8 AU.

We thank Bill Tomlinson, Tom Booker, and Don Mahoney at SwRI, Richard Sturtz of Xybion, Inc., and Vic Genau for their diligent attention to detail and care in building and qualifying SWUIS for flight. We thank Al Ong, Jackie Prewitt, Barbara Smith, and the entire JSC flight control team for their great help in planning and executing the SWUIS observations. We also wish to thank Mission Specialist Steve Robinson and the entire STS-85 flight crew for conducting the actual observations of Hale-Bopp with SWUIS. Both referee David Schleicher and Dan Durda provided helpful critiques of this manuscript. This work was supported by NASA's Office of Space Science under the Planetary Astronomy and Suborbital Research Program (NAG 5-5098), NASA Planetary Astronomy grant NAG 5-7312, JPL contract 960549, and JHU/APL contract 759577.

REFERENCES

A'Hearn, M. F., Millis, R. L., Schleicher, D. G., Osip, D. J., & Birch, P. V. 1995, Icarus, 118, 223

A'Hearn, M. F., Schleicher, D. G., Feldman, P. D., Millis, R. L., & Thompson, D. T. 1984, AJ, 89, 589

Biver, N., et al. 1997, Science, 275, 1915

———. 1999, Earth Moon Planets, in press

Budzien, S. A., Festou, M. C., & Feldman, P. D. 1994, Icarus, 95, 65

Colom, P., Gérard, E., Crovisier, J., Bockelée-Morvan, D., Biver, N., & Rauer, H. 1999, Earth, Moon, Planets, in press

Despois, D., Gerárd, E., Crovisier, J., & Kazes, I. 1981, A&A, 99, 320

Farnham, T. L., & Schleicher, D. G. 1999, Icarus, submitted

Feldman, P. D. 1982, in Comets, ed. L. L. Wilkening (Tucson: Univ. Arizona Press), 461

———. 1991, in Comets in the Post-Halley Era, ed. R. Newburn, M. Neugebauer, & J. Rahe (Dordrecht: Kluwer), 141

Festou, M. C. 1981. A&A, 96, 69

Festou, M. C., Rickman, H., & West, R. 1993a, A&A Rev., 4, 363

———. 1993b, A&A Rev., 5, 37

Kurucz, R. L. 1992, in IAU Symp. 149, The Stellar Populations of Galaxies, ed. B. Barbuy & A. Renzini (Dordrecht: Kluwer), 225

Millis, R., Schleicher, D. G., & Farnham, T. 1997, BAAS, 29, 1035

Schleicher, D. G., & A'Hearn, M. F. 1988, ApJ, 331, 1058

Schleicher, D. G., & Farnham, T. 1997, Science, 275 1913

Slater, D. C., et al. 1999, in Proc. Space Technology and Applications International Forum (STAIF-99) (Albuquerque: Univ. New Mexico), in press

Stern, S. A. 1999, in The Origin and Composition of Cometary Material, ed. K. Altwegg et al. (Bern: ISSI), in press

Weaver, H. A., Feldman, P. D., A'Hearn, M. F., Arpigny, C., Brandt, J. C., & Stern, S. A. 1999, Icarus, in press